Density Embedded VB/MM: A Hybrid ab Initio VB/MM with Electrostatic Embedding

Avital Sharir-Ivry,[†] Hadar A. Crown,[†] Wei Wu,[‡] and Avital Shurki*[,†,§]

Department of Medicinal Chemistry and Natural Products, The Lise Meitner-Minerva Center for Computational Quantum Chemistry, School of Pharmacy, The Hebrew University of Jerusalem, Jerusalem 91120, Israel, and Department of Chemistry, Center for Theoretical Chemistry and State Key Laboratory of Physical Chemistry of Solid Surfaces, Xiamen University, Xiamen, Fujian 361005, China

Received: October 28, 2007; In Final Form: December 10, 2007

A hybrid QM/MM method that combines ab initio valence-bond (VB) with molecular mechanics (MM) is presented. The method utilizes the ab initio VB approach to describe the reactive fragments and MM to describe the environment thus allows VB calculations of reactions in large biological systems. The method, termed density embedded VB/MM (DE-VB/MM), is an extension of the recently developed VB/MM method. It involves calculation of the electrostatic interaction between the reactive fragments and their environment using the electrostatic embedding scheme. Namely, the electrostatic interactions are represented as one-electron integrals in the ab initio VB Hamiltonian, hence taking into account the wave function polarization of the reactive fragments due to the environment. Moreover, the assumptions that were utilized in an earlier version of the method, VB/MM, to formulate the electrostatic interactions effect on the off-diagonal matrix elements are no longer required in the DE-VB/MM methodology. Using DE-VB/MM, one can calculate, in addition to the adiabatic ground state reaction profile, the energy of the diabatic VB configurations as well as the VB state correlation diagram for the reaction. The abilities of the method are exemplified on the identity S_N2 reaction of a chloride anion with methyl chloride in aqueous solution. Both the VB configurations diagram and the state correlation diagram are presented. The results are shown to be in very good agreement with both experimental and other computational data, suggesting that DE-VB/MM is a proper method for application to different reactivity problems in biological systems.

Introduction

An accurate potential energy surface (PES) is a fundamental requirement for reliable calculations of many chemical properties. Quantum chemistry is suitable for describing PES of relatively small systems in the gas phase, and desired accuracy can be achieved by increasing the level of the calculation. Similarly, studies of chemical reactions in biological systems are based on hybrid quantum mechanical molecular mechanical (QM/MM) methodologies[1−19] which solve the issue of computation time vs accuracy by changing both the size and the level of the QM part in the calculation.

The valence bond approach (VB) is well-suited to understanding chemical reactivity.[20,21] Hence, many QM/MM methods aiming at understanding reactions in biological systems have been developed using VB concepts and methodology.[15,16,22−46]

Warshel's empirical valence bond (EVB) approach describes each one of the diabatic VB states (e.g., reactants and products) using classical PES.[16,22−24] The overall adiabatic PES is eventually obtained by mixing these diabatic states by an off-diagonal matrix element, H_{ij}, that represents the interaction between them. The EVB approach uses a simple exponential function to describe this interaction while adjusting it to reproduce the experimental (or ab initio) reaction barrier. This adjusted function is then used to describe the PES of the same reaction in a different environment. The EVB describes well the energetics of the PES at the critical points (reactants TS and products), but the overall shape of the profile and the vibrations of the TS are not necessarily well defined. Hence, Chang and Miller[25,26] followed by others have developed various methods to obtain H_{ij} by fitting the empirical potential to an ab initio or density functional (DFT) potential.[25−28] Additional developments in this direction led to the multiconfiguration molecular-mechanics (MCMM) which introduced the Shepard interpolation. This allowed fitting of H_{ij} not only at the critical points but along the global PES.[29,30] Furthermore, H_{ij} fitting in certain levels of MCMM is based on QM/MM potentials rather than QM potential,[31] allowing studies of very large reactive systems. Other developments such as the extended EVB[32,33] and the multistate EVB[34,35] generalized the Chang and Miller formalism to calculation of various VB states.

A slightly different approach was used by Truhlar et al. in the combined valence bond molecular mechanics (CVBMM).[36] Similar to the EVB, the QM part in the CVBMM utilizes some parametrized VB potential. However, the coupling between the QM part and the MM part in CVBMM is calculated directly with the adiabatic state as in the various MO based QM/MM methods rather than with each one of the diabatic states separately.[36]

A very different approach was suggested by Bernardi et al. in their molecular mechanics valence bond (MMVB) method.[15,37,38] Unlike most QM/MM methods where certain atoms (regions of the system) define the QM part while other atoms define the MM part, MMVB involves definition of certain active orbitals as the QM part while the rest of the system is described with

* Corresponding author: E-mail: avitalsh@ekmd.huji.ac.il. Phone: +972-2-675-8696. Fax: +972-2-675-7076.
[†] The Hebrew University of Jerusalem.
[‡] Xiamen University.
[§] Affiliated with the David R. Bloom Center for Pharmacy at the Hebrew University.

10.1021/jp710395b CCC: $40.75
Published on Web 02/23/2008

MM. A certain atom can therefore belong to both the QM and the MM parts. Moreover, various integrals of the QM Hamiltonian are parametrized to fit ab initio CASSCF calculations. The method is currently limited to hydrocarbons since extension to heteroatoms that may involve more then one active orbital is not straightforward.

All these methods involve a quantum part, which is either fully or partially described by parameter based PES and thus requires parametrization, which can be a tedious task. A different class of VB based methods for large biological systems therefore has evolved. One such method is the molecular orbital valence bond (MOVB) of Gao and Mo.[39−41] The method is based on a block-localized wave function approach to define the diabatic states, which are then mixed using a configuration interaction type of calculation. The method is based on a single determinant treatment and, thus, allows its QM part to have the accuracy of either HF or DFT calculations.[39,40,47] A different method is based on the constrained and frozen density functional (CDFT and FDFT).[42−44,48] This method uses constraints to localize the electron density on various prechosen fragments. Calculation with the constraints allows the description of different diabatic states while calculation without the constraint results in the adiabatic state, providing a full VB description of the system. Yet, due to the requirement of orthogonality between the orbitals of the various fragments, it is mainly useful when the fragments are distant from each other. Finally, Wu et al. have developed the first ab initio VB based method: the VBPCM, which combines VB with the polarizable continuum model, allowing therefore inclusion of solvent effects.[45] This method, however, cannot be utilized to describe reactivity in biological systems like proteins.

Recently an ab initio VB/MM method has been developed.[46] This method described the QM part using ab initio VB while inclusion of the environment was achieved by implementing point-charge (also called mechanical) embedding for each diabatic state separately.[46] Mixing of the diabatic states guarantees some wave function polarization due to the environment. However, a VB/MM method with a better embedding scheme is important for a description which involves fewer approximations. The present paper describes a further development of ab initio VB/MM (to be termed here density embedded VB/MM (DE-VB/MM)), which involves mainly improvement of the embedding scheme from point-charge (mechanical) to electrostatic embedding.[6] We will first describe the method and then illustrate its implementation to the identity S_N2 reaction of a chloride anion with methyl chloride in aqueous solution. It is shown that the method gives very good agreement with experimental data.

Method: Model Description

Hybrid QM/MM methods involve a small part of the system (the reactive subsystem) which is treated quantum mechanically, while the rest of the system (the environment) is described by a classical force field. The overall Hamiltonian H consists of three terms:

$$H = H_{QM} + H_{MM} + H_{QM/MM} \tag{1}$$

where H_{QM} and H_{MM} are Hamiltonian operators that describe the interactions within the QM and MM parts of the system, respectively and $H_{QM/MM}$ accounts for interactions between the QM and MM subsystems.

In the VB/MM approach, the reactive subsystem is defined by using N valence bond electronic configurations Φ_i, that are sufficient to describe the system, where each VB configuration corresponds to a definite arrangement of the electrons. Thus, the overall wave function at any given geometry is defined as a linear combination of the different VB configurations:

$$\Psi_{VB} = \sum_{i}^{N} c_i \Phi_i \tag{2}$$

For the simplicity of the following description we will consider only two VB configurations (i.e., $N = 2$; e.g., reactant and product covalent configurations) but the method is general and the same can be applied for any number of configurations. Following the Born−Oppenheimer approximation, at any given geometry the potential energy ϵ is approximated by the lowest eigenvalue of the secular equation:

$$\begin{pmatrix} H_{11} - \epsilon S_{11} & H_{12} - \epsilon S_{12} \\ H_{12} - \epsilon S_{12} & H_{22} - \epsilon S_{22} \end{pmatrix} \begin{pmatrix} c_1 \\ c_2 \end{pmatrix} = 0 \tag{3}$$

where the H_{11} and H_{22} matrix elements are the energies of the VB configurations Φ_1 and Φ_2 respectively, H_{12} and S_{12} are, respectively, the resonance integral and the overlap integral between the respective VB configurations (Φ_1 and Φ_2), while the intrinsic overlap $S_{11} = S_{22} = 1$ due to normalization.

As specified previously, in any QM/MM calculation the reactive subsystem is described at the QM level whereas the environment is treated at the MM level. The electrostatic interaction between the reactive system and its environment can be calculated classically, at the MM level in the point charge (mechanical) embedding scheme,[6,49,50] or modeled as one electron operators that enter the QM Hamiltonian in the electrostatic embedding scheme.[6,50,51] The early VB/MM utilized point charge (mechanical) embedding for each one of the VB configurations separately. DE-VB/MM, however, employs the electrostatic embedding scheme. That is, the electrostatic part of the interaction Hamiltonian between the QM reactive subsystem and the MM environment is included in the optimization of the reactive subsystem's wave function. This is done by incorporating the one-electron integral term, resulting from the environment electric field, in the Hamiltonian of the reactive system as follows:

$$H'_{QM} = H^0_{QM} + V^{ele}_{QM/MM} \tag{4}$$

where, H^0_{QM} is the Hamiltonian of the isolated reactive subsystem and $V^{ele}_{QM/MM}$ accounts for the electrostatic contributions from all the environment's charges.[52,53]

The remaining of $H_{QM/MM}$, involving van der Waals (VdW) type of nonbonded interactions between the reactive subsystem and the environment, was calculated classically. The VdW radius of a charged atom is expected to be different from that of a neutral atom. Therefore, similar to VB/MM, these VdW nonbonded interactions were calculated for each VB configuration separately using the Lennard-Jones formulation:

$$H^{LJ}_{QM/MM,ii} = \sum_{\substack{k,l \\ \text{not bonded} \\ \text{in } \Phi_i}} \left(\epsilon^* \left[\left(\frac{r^*}{r_{kl}} \right)^{12} - 2 \left(\frac{r^*}{r_{kl}} \right)^{6} \right] \right) \tag{5}$$

where $H^{LJ}_{QM/MM,ii}$ is the VdW interaction of the ith VB configuration with its surroundings and k and l run over the QM nuclei and MM atoms, respectively. It is noted that k and l should be such that they are not bonded in the Φ_i VB configuration. Currently, our method deals only with systems where the

reactive subsystem is not covalently bonded to its environment, in which case, together, k and l run over all the system's atoms. ϵ^* and r^* are the Lennard-Jones parameters describing the attraction well depth and the equilibrium distance of the interaction between the QM nuclei k and MM atom l.

Thus, the evaluation of the overall energy of the ith diagonal element utilizes the following equation:

$$H_{ii} = H'_{\mathrm{QM},ii} + H^{\mathrm{LJ}}_{\mathrm{QM/MM},ii} \tag{6}$$

where $H'_{\mathrm{QM},ii}$ is the quantum diagonal energy that includes also the electrostatic interaction and $H^{\mathrm{LJ}}_{\mathrm{QM/MM},ii}$ is the respective VdW interaction.

In order to evaluate the off-diagonal elements we assumed that both the reduced resonance integral, β_{ij}, and the overlap, S_{ij}, are invariant to the VdW interactions of the reactive subsystem with its environment. For any $H_{ii} = H_{jj}$, β_{ij} is given by the following formula (see Supporting Information for derivation of this formula):

$$\beta_{ij} = H_{ij} - \frac{1}{2}(H_{ii} + H_{jj})S_{ij} \tag{7}$$

We note here that β_{ij} is more often referred to as H_{ij} for cases with no overlap between the different configurations, i.e., $S_{ij} = 0$. The assumption that this reduced resonance integral does not depend on the surroundings laid the foundations of various established methods, such as the EVB, and was demonstrated recently to be a rather good approximation.[42] As for the approximation with regard to the overlap, the overall wave function is largely affected by the environment. This, however, is a result of changes in the relative stabilization of the various electronic configurations and not due to changes in the wave function of each electronic configuration separately. In fact, the effect of the environment on the wave function of each VB configuration separately and therefore the overlap between any two VB configurations is expected to be negligible. Most methods suppose zero overlap between the various VB configurations.[16,22,23,25−30,32−35] Our method calculates both the exact overlap and reduced resonance integral for the reactive system including the electrostatic effect of the surroundings. It then assumes invariance of these integrals only with respect to the effect of the VdW interactions of the reactive subsystem with its environment.

Using these approximations, one can easily derive the following equation (see Supporting Information for more details) to evaluate the off-diagonal elements of two configurations whose relative energies are equal ($H_{ii} = H_{jj}$):

$$H_{ij} = H'_{\mathrm{QM},ij} + \frac{1}{2}(H^{\mathrm{LJ}}_{\mathrm{QM/MM},ii} + H^{\mathrm{LJ}}_{\mathrm{QM/MM},jj})S'_{\mathrm{QM},ij} \tag{8}$$

where $H'_{\mathrm{QM},ij}$ is the quantum off-diagonal resonance energy that includes electrostatic interactions with the environment, $H^{\mathrm{LJ}}_{\mathrm{QM/MM},kk}$ is the respective VdW interaction of Φ_k with its surroundings and $S'_{\mathrm{QM},ij}$ is the overlap between Φ_i and Φ_j as obtained in the quantum calculation for the reactive subsystem with an external field created by the environment's point charges. The same equation was then used to approximate H_{ij} for every point along the entire potential energy surface.[54]

Finally, the eigenvalue problem with the new matrix elements as defined in eqs 6 and 8 is solved, leading to energy and wave function that account for the various effects of the surroundings. The environment may have a significant effect on the overall wave function of the system which in turn can affect the environment (e.g., a wave function usually becomes more polarized in aqueous solution, which in turn causes the water molecules to reorganize accordingly). Thus, the procedure is repeated iteratively, with configurations that are obtained by equilibrating the system with the newly obtained wave function, until changes in the wave function between two sequential iterations are small. Scheme 1 summarizes the various steps of the DE-VB/MM method.

Computational Details

DE-VB/MM couples ab initio VB and molecular mechanical calculations. The Xiamen VB (XMVB) program package[56,57] served us for the ab initio VB calculations whereas MOLARIS[58,59] was used for the dynamics and all the force-field calculations. To allow actual DE-VB/MM calculations, MOLARIS has been modified to treat nonorthogonal VB states and an interface program that serves as a linkage between the two packages (MOLARIS and XMVB) was written.

Quantum Calculations. Reactants (RS), products (PS), and transition state (TS) gas-phase geometries were optimized at the HF/6-31G* level, while other geometries along the reaction profile were determined by dividing the geometrical changes from reactants to the TS and from the TS to the products into 28 equal fractions which were appended gradually to form a complete profile.

The accuracy of the results largely depends on both the basis set and the quantum mechanical VB level chosen, and an improved level of accuracy can be obtained by rigorously improving these two aspects. In this study the VB calculations utilized two approaches: the valence bond self-consistent field (VBSCF) and the breathing orbital valence bond (BOVB). The VBSCF approach describes different configurations with the same set of orbitals which are allowed to optimize in order to minimize the total energy. The BOVB approach on the other hand uses different orbital sets to describe the different VB configurations, and the various orbital sets are mutually allowed to optimize.[60,61] The inner core electrons of the various atoms (1s for carbon and 1s, 2s and 2p for chlorine) were frozen at the Hartree−Fock (HF) level, while the remaining 22 electrons were explicitly calculated in the VB scheme. π orbitals were allowed to delocalize while σ-type orbital were kept strictly localized on the respective fragments. The calculations employed the 6-31G* basis set. Both VBSCF and BOVB involved the spin-free formulation.[57,62]

The electrostatic interaction of the solvent with the reacting fragments was determined by considering the solvent atoms as point charges and including the solute−solvent one electron integrals $V^{\mathrm{ele}}_{\mathrm{QM/MM}}$ in the one electron matrix. This way, explicit solvent effects are incorporated in both the diagonal and off-diagonal matrix elements similar to the MOVB calculations.[39,40] Finally VdW effects were introduced using the classical VdW interaction following eqs 5, 6 and 8.

Classical Simulations. All simulations have been performed according to the standard simulation technique starting from some initial configuration as a guess for the solvent molecules and allowing the trajectories to evolve in the MD runs and accommodate to the electronic structure of the reacting fragments. This electronic structure is defined as a linear combination of the different VB configurations multiplied by their corresponding weights in the wave function. The initial guess for the weights was obtained from gas-phase calculations of the reactive system. A 50 ps relaxation of the solvent coordinates with a fixed solute geometry was carried out for each point along the reaction coordinate. A single point DE-VB/MM calculation

SCHEME 1: Schematic Diagram of the DE-VB/MM Method[a]

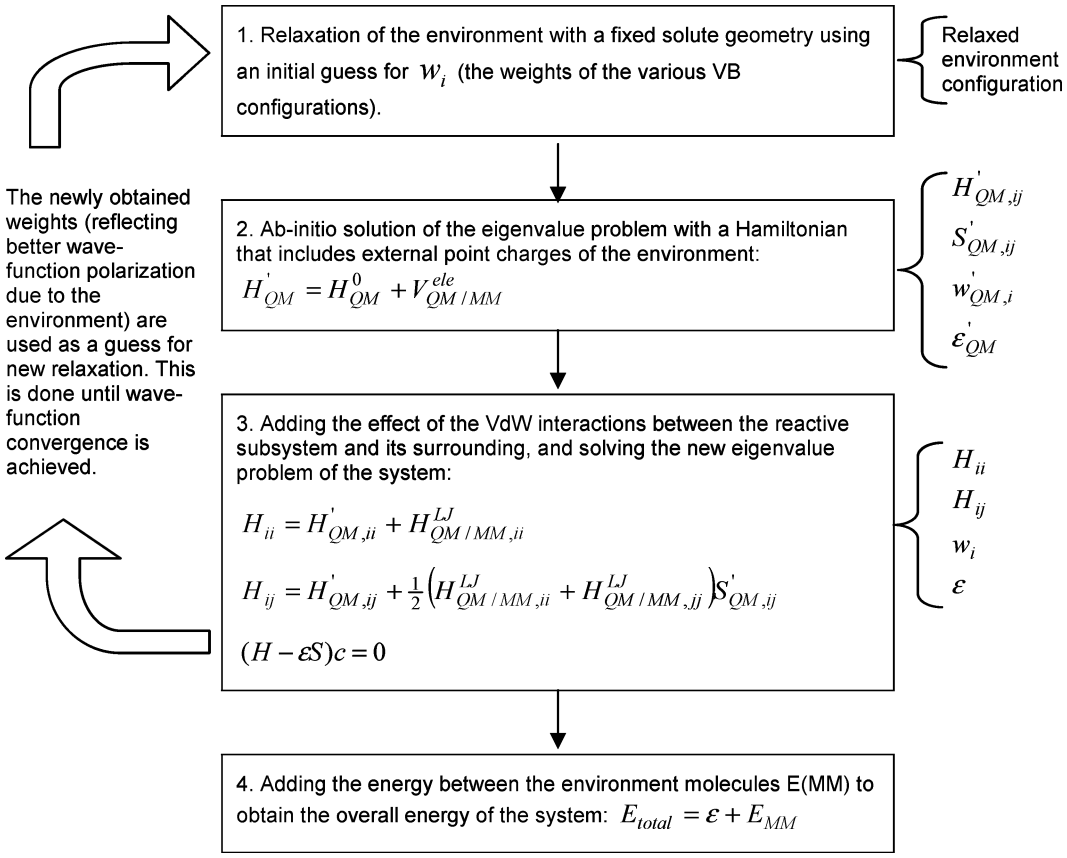

[a] Outputs from the corresponding step are indicated by curly brackets. The diagram describes the various calculation steps for a single frozen solute geometry. Furthermore, the diagram describes the calculation done on a single relaxed environment configuration, where for the complete calculation, several relaxed configurations are considered and the average is used as the result.

of the relaxed system was then performed, resulting in new weights for the diabatic VB configurations. These new weights were then used for a subsequent relaxation, and the process was repeated until $\Delta\omega_i$, the difference in the weights between two sequential relaxations, reached a minimum value (up to 0.05). Once convergence of the wave function in the solution was obtained, we collected 50 different solvent configurations of the system for each solute geometry along the reaction coordinate. This was done by continuously equilibrating the system at each solute geometry and performing a DE-VB/MM calculation after every 1 ps in an overall 50 ps simulation. Finally, we followed the potential of mean force (PMF) protocol[63−66] using the free energy perturbation (FEP) theory[67,68] to obtain the free energy profile of the reaction. Both forward and backward calculations were carried out, and the average of the two is presented.

Fundamental for all simulations is the standard surface constrained all-atom solvent (SCAAS) simulation technique model[63] with the local reaction field (LRF) long-range treatment.[69] The overall system is spherical and divided into several regions: region I contained the reacting fragments $CH_3-Cl + Cl^-$; region II comprised the explicit water molecules up to a radius of 18 Å and is represented with the standard ENZYMIX force field parameters.[58,59] A detailed description of the force-field parameters for the reacting fragments at the various VB configurations is given in Supporting Information. Finally, the system was embedded in a 2 Å shell of Langevin dipoles and a dielectric continuum simulating the bulk solvation. All the simulations were carried out at 300 K and involved 1 fs time step.

Results and Discussion

The reaction chosen for this study is the following identity nucleophilic substitution:

$$Cl^- + CH_3-Cl \rightarrow Cl-CH_3 + Cl^- \qquad (9)$$

Four valence electrons in three orbitals participate in the bond-breaking/bond-formation during this chemical reaction. Therefore, a full VB description involves six different valence bond configurations **1**−**6**. **1** and **2** are the two covalent configurations, the reactants Φ^R_{cov} and the products Φ^P_{cov}, respectively; **3** represents the triple-ionic configuration (ionic hereafter), consisting of carbocation and two negatively charged chlorine ions, Φ_{ion}; configurations **4**−**6** exhibit electronic distribution which involves a carbanion while configuration **4** involves also a long bond between the two chlorine atoms Φ_{LB} and configurations **5** and **6** involve one positively charged chlorine ion. Both methyl chloride and the chloride ion define the reactive subsystem whereas the solvent molecules define the environment.

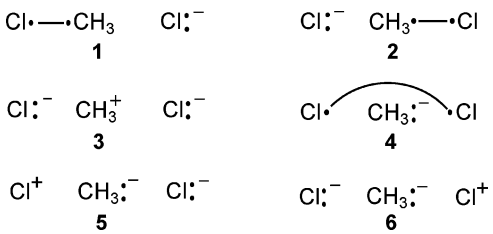

Gao et al. showed in their work that the identical S_N2 reaction is well described by a geometrical reaction coordinate conclud-

TABLE 1: Experimental and Calculated Values of Gas Phase as Well as Aqueous Solution Reaction Barriers for the Reaction $Cl^- + CH_3-Cl \rightarrow Cl-CH_3 + Cl^-$[a]

level	$\Delta g^{\ddagger}$
Gas Phase	
VBSCF(3)	17.0
VBSCF(6)	19.5
BOVB(3)	9.9
BOVB(6)	11.4
experimental	10.2[b] (8.6[c])
Solvent	
DE-BOVB(3)/MM	24.6
experimental	26.5[d]

[a] All calculations utilized the 6-31G(d) basis set, barriers are in kcal/mol. [b] See refs 72, 73. [c] See ref 74. [d] See ref 75.

ing that in this case inclusion of the solvent in the reaction coordinate does not have a critical effect.[40] Thus, in this work we chose to use a geometrical reaction coordinate throughout the calculations. Yet, we graphically presented the results along $\Delta\epsilon$ where $\Delta\epsilon$ is defined as the energy difference between the energies of the covalent reactants Φ^{R}_{cov} and products Φ^{P}_{cov} VB configurations **1** and **2**, respectively.

$$\Delta\epsilon = \epsilon_1 - \epsilon_2 \tag{10}$$

Table 1 summarizes the calculated reaction barriers both in vacuum and in aqueous solution and compares them to experimental values. Due to the sampling problem, when choosing a level of calculation for the aqueous system it is important to compromise between two factors: computational cost and accuracy. Since the accuracy of aqueous calculations is likely to be affected by the accuracy of gas-phase calculations, various levels of VB calculations were first tested for the gas-phase calculations differing by the number of VB configurations as well as the amount of correlation considered. Looking at the table it is seen that in general the BOVB results give a good agreement with the experimental results while VBSCF give relatively high barriers, suggesting that for this reaction dynamic correlation is important. Furthermore, comparing the results obtained with all the 6 VB configurations (entries 2, 4) to those obtained with configurations **1**−**3** only (entries 1, 3) it is seen that there is a relatively small difference. As mentioned previously configurations **4**−**6** exhibit electronic distribution which involves a carbanion and in configurations **5** and **6** also a positively charged chlorine ion. These VB configurations are, therefore, expected to be very high in energy, and their contribution is expected to be small. Our calculations demonstrate in agreement with previous findings[40,70,71] that the overall effect of configurations **4**−**6** is indeed small being ∼1−2 kcal/mol regardless of the method used. Therefore the BOVB(3) level was chosen for further studies of the system in solution where 3 stands for configurations **1**−**3**.

The last two entries in the table represent the barrier for the reaction in solution. As expected the barrier increased due to the better solvation of the reactants and products compared to the TS, which is less polar in this reaction. The calculations predict an increase of ∼15 kcal/mol, in very good agreement with the ∼16 kcal/mol anticipated by experiment, suggesting that the DE-VB/MM method is well defined. Furthermore, our results compare well with results obtained by the VBPCM approach (26.8 kcal/mol) which utilized the BOVB approach with all 6 VB configurations.[45,70]

Despite the symmetric character of the reaction we calculated the overall reaction profile rather than only one-half of it, as is sometimes done in these cases. This allowed us to get additional assessment of the accuracy of the calculations. Table 2 lists the weights of configurations **1**−**3** both in the gas phase and in solution. The weights are given for five different sequential geometries along the reaction coordinate: the critical geometries of reactants (A), TS (C) and products (E), and two additional geometries in between (B, D). The geometries were chosen to be such that (A) and (B) are mirror images of the geometries (E) and (D), respectively. Looking at the table one can see, in agreement with previous studies,[70] that the solvent has a substantial effect on the TS's wave function (entry 3) whose ionic character increases considerably (0.56 compared to only 0.46 in the gas phase) due to the presence of the solvent. The wave function of both the reactants and products on the other hand (entries 1 and 5) is affected to a much lesser extent. We note with this respect that, in this particular reaction, in general there is a fairly small overall stabilization of the ionic configuration relative to the covalent one, despite the polar solvent. This, however, results from the fact that each one of the covalent configurations already involves some ionic character (the negatively charged nucleophile in the reactant configuration or the negatively charged leaving group in the product configuration) that also stabilizes considerably in polar solution.

Further inspection of the TS weights (entry 3) reveals a minor discrepancy in the description of the solution wave function. While the gas-phase wave function exhibits perfectly symmetric wave function with identical contributions of both reactant and product covalent configurations, Φ^{R}_{cov} and Φ^{P}_{cov}, this expected symmetry is slightly corrupted in our reported values in solution. Here Φ^{P}_{cov} seems to have a somewhat larger contribution to the overall wave function than Φ^{R}_{cov}. Moreover, comparing the weights for geometry (B) to those presented for geometry (D) one finds additional discrepancy. These two geometries are mirror images of one another and as such the weights of Φ^{R}_{cov} and Φ^{P}_{cov} for geometry (B) should be identical to those of Φ^{P}_{cov} and Φ^{R}_{cov} for geometry (D), respectively. Yet, the weights are not identical and in contrast to the TS, geometry (D) favors Φ^{R}_{cov} over Φ^{P}_{cov} compared to geometry (B). Finally, comparing the weights for the reactant's geometry (A) to those obtained for the product's geometry (E) there is virtually no difference. Additional discrepancies in the weights are found in various geometries along the reaction coordinate which are presented in Supporting Information (Table 4S).

These discrepancies are not consistent in size and direction and fluctuate for the different geometries along the reaction coordinate, indicating that this imperfect symmetry of the wave function is due to a sampling problem. We note, however, that these deviations from a symmetric description are very small, suggesting that the method is quite robust with respect to wave function prediction.

Figure 1 displays the potential energy curves for the reaction in vacuum (a) and in aqueous solution (b). The adiabatic ground-state profile is shown in bold lines while the individual nonvariational diabatic profiles describing VB configurations **1**−**3** are presented in plain lines. The energy of the ion−dipole complex geometry in vacuum served as a reference for the energies both in vacuum and in solution.

Looking at Figure 1 and particularly at the curves of the diabatic VB configurations, it is seen that while the gas-phase curves are symmetric, as one would expect, in solution the situation is different. Namely, in solution the two covalent states, which are supposed to be a mirror image of one another, are not completely symmetric. Similarly, the curve of the ionic configuration is also distorted and somewhat distant from

TABLE 2: Calculated Gas Phase and Solution Weights of Configurations 1−3 in Various Geometries along the Reaction Profile[a]

geometry	$(r_1;r_2)$[b]	$w_{gas}(\Phi^R_{cov}/\Phi^P_{cov}/\Phi_{ion})$	$w_{solution}(\Phi^R_{cov}/\Phi^P_{cov}/\Phi_{ion})$
A	(1.907;3.138)	0.602/0.023/0.374	0.634/0.005/0.360
B	(2.344;2.446)	0.310/0.227/0.462	0.314/0.138/0.548
C	(2.383;2.383)	0.268/0.268/0.463	0.217/0.222/0.560
D	(2.446;2.343)	0.227/0.310/0.462	0.147/0.295/0.557
E	(3.138;1.907)	0.023/0.602/0.374	0.005/0.633/0.361

[a] Weights are calculated according to the Coulson−Chirgwin formula.[76] [b] r_1 and r_2 reflect the distance in Å between the CH_3 moiety and the leaving group or the nucleophile, respectively.

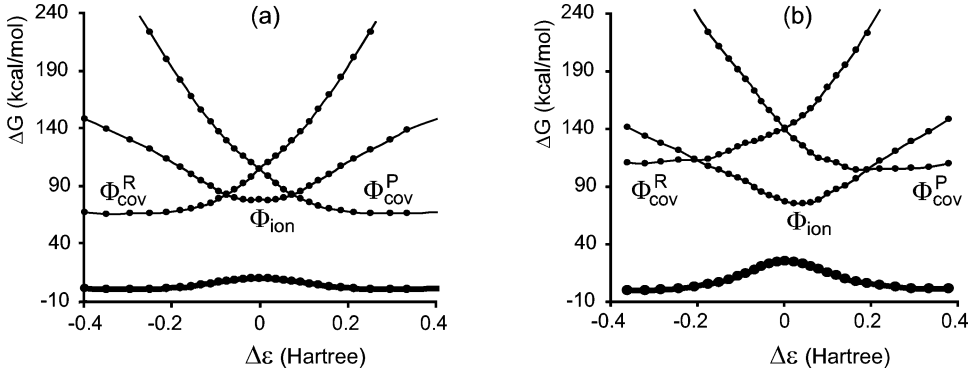

Figure 1. S_N2 reaction profile in vacuum (a) and in solution (b). Plain lines depict the energy of the diabatic VB configurations (Φ^R_{cov},Φ^P_{cov}, and Φ_{ion}), whereas bold lines depict the adiabatic ground state. Energies are presented relative to the ion−molecule complex in the gas phase and relative to the energy of the gas-phase ion−molecule complex geometry in solution.

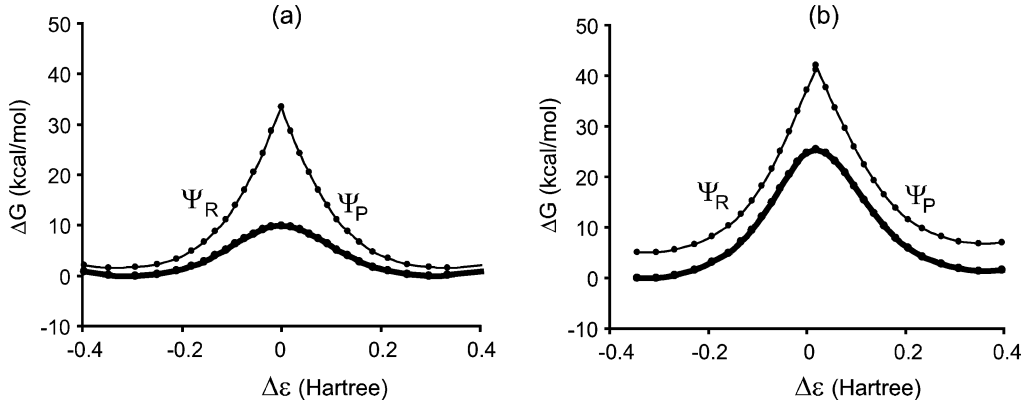

Figure 2. State correlation diagram for the S_N2 reaction in vacuum (a) and in solution (b). Plain lines depict the energy of the diabatic VB states (Ψ^R,Ψ^P), whereas bold lines depict the adiabatic ground state. Energies are presented relative to the ion−molecule complex in the gas phase and relative to the energy of the gas-phase ion−molecule complex geometry in solution.

symmetric. As a result, the adiabatic profile of the solution reaction is slightly deformed suggesting incorrectly that the products are 1.6 kcal/mol higher than the reactants. This misshaped behavior of the various curves is a result of the PMF procedure. A proper description of the curves largely depends on both the number of frames within the PMF scheme and the amount of sampled configurations. The larger the overall energy span of the curve, the larger is the number of frames and sampled configurations required to properly describe it within the PMF scheme. Thus, a better description should simply involve a greater number of both frames and configurations sampled within each frame. Yet, we note here with this respect that this deviation is very small, suggesting that the DE-VB/MM method is quite robust.

Finally, similar to the VBPCM, the DE-VB/MM approach allows calculation of the VB state correlation diagrams (VB-SCD) in solution. Here, instead of the VB configurations we follow the energy of the two diabatic states; the reactant's ψ_R, and product's ψ_P states which are linear combinations of several VB configurations. This, in turn, allows one to evaluate the resonance energy at various points along the reaction and in particular at the transition state, where it is defined as the energy difference between the crossing point of the two states and the actual ground-state energy at that point.

Figure 2 represents the reaction profile (bold lines) along with the two diabatic states (plain lines), up to the point where they intersect. The curves of both gas-phase and solution reaction are presented. Analysis of these VBSCD indicates that the resonance energy at the transition state is calculated to be 23.6 kcal/mol in gas phase and 16.2 kcal/mol in aqueous solution. This reduction in the resonance energy due to changes in the environment suggests that the solvent affects both the overall energy of the states and their shared interaction. As was explained in previous studies, this reduction in the resonance energy is a result of an increased ionic contribution in aqueous solution relative to gas phase, at the TS geometry.[45,70]

The resonance energy obtained here is in relatively good agreement with the values obtained by Shaik and co-workers.[70] In their work they reported resonance energies of 21.2 and 16.9 kcal/mol for gas phase and aqueous solution, respectively,

resulting in an overall reduction of about 4.7 kcal/mol.[70] Furthermore, using several approximations, Shaik et al. derived two equations, which predicted similar values of resonance energies.[70] Our calculations resulted with the same overall trend and with similar absolute values, though with somewhat higher reduction in the resonance energy (7.4 kcal/mol). The reactant's state should be a mixture of configurations **1**, **3**, **4** and **5** while the product's state is a mixture of configurations **2**, **3**, **4** and **6**. However, our calculations involved only configurations **1**−**3**, hence, the reactants and products states were described, respectively, as a linear combination of VB configurations **1**, **3** and **2**, **3** only. This, most likely, explains the differences between our results and the results obtained by Shaik et al., who used the proper number of VB configurations.[70] Still it should be emphasized that the differences are small and as a whole there is a good agreement with these results.

Concluding Remarks

A new hybrid QM/MM method, DE-VB/MM, in which the QM part is described by ab initio valence bond approach was developed. The method combines ab initio VB with MM using ideas taken from the EVB approach. That is, the interaction with the solvent is calculated separately with each diabatic state. Furthermore, instead of the point-charge (mechanical) embedding scheme, which was utilized in VB/MM, DE-VB/MM employs the electrostatic embedding scheme, which involves fewer approximations. More specifically, while VB/MM calculates the electrostatic interaction between the reacting system and the environment classically (a scheme which involves various approximations for evaluating the off-diagonal element), DE-VB/MM introduces a one-electron term which represents the interaction between the environment and the reacting system into the QM Hamiltonian. This eliminates the need for approximating the effect of the electrostatic interaction between the QM and MM regions on the off-diagonal element within DE-VB/MM.

The method was tested by studying the identity S_N2 reaction $Cl^- + CH_3{-}Cl \rightarrow Cl{-}CH_3 + Cl^-$ and comparing the results obtained in the gas phase to those obtained in solution and to available experimental data. The method was shown to be successful in predicting the reaction profile including the reaction barrier. Furthermore, it was shown to be able to calculate both the overall wave function and the resonance energies in a relatively good agreemnet with the VBPCM method. Yet, the advantage of DE-VB/MM over the VBPCM is that it utilizes force-field to describe the environment rather than a continuum model. Therefore, while the VBPCM method is limited to the description of reactions in solvents, DE-VB/MM should also be capable of calculating reactions within proteins. Future applications of the method to biological systems therefore await us.

Acknowledgment. The research was supported by The Israel Science Foundation (Grants No. 1317/05 and 1320/05) and by the Human Frontier Science Program HSFP (Grant No. RGY0068/2006-C102). Research at XMU is supported by the Natural Science Foundation of China (No. 20533020) and The National Basic Research Program of China (2004CB719902).

Supporting Information Available: Derivation of eqs 7 and 8 along with detailed explanation and justification of the updated approximation for H_{ij}, a detailed description of the force field parameters used in the calculations and a table listing gas-phase and solution weights in additional geometries. This material is available free of charge via the Internet at http://pubs.acs.org.

References and Notes

(1) Warshel, A.; Levitt, M. *J. Mol. Biol.* **1976**, *103*, 227.
(2) Warshel, A. *Annu. Rev. Biophys. Biomol. Struct.* **2003**, *32*, 425.
(3) Field, M. J.; Bash, P. A.; Karplus, M. *J. Comput. Chem.* **1990**, *11*, 700.
(4) Field, M. *J. Comput. Chem.* **2002**, *23*, 48.
(5) Cui, Q.; Elstner, M.; Kaxiras, E.; Frauenheim, T.; Karplus, M. *J. Phys. Chem. B* **2001**, *105*, 569.
(6) Bakowies, D.; Thiel, W. *J. Phys. Chem* **1996**, *100*, 10580.
(7) Friesner, R. A.; Beachy, M. D. *Curr. Opin. Struct. Biol.* **1998**, *8*, 257.
(8) Monard, G.; Merz, K. M., Jr. *Acc. Chem. Res.* **1999**, *32*, 904.
(9) Gao, J. *Reviews in Computational Chemistry*; VCH: New York, 1995; Vol. 7.
(10) Vasilyev, V. V.; Bliznyuk, A. A.; Voityuk, A. A. *Int. J. Quantum Chem.* **1992**, *44*, 897.
(11) Théry, V.; Rinaldi, D.; Rivail, J.-L.; Maigret, B.; Ferenczy, G. G. *J. Comput. Chem.* **1994**, *15*, 269.
(12) Thompson, M. A.; Glendening, E. D.; Feller, D. *J. Phys. Chem.* **1994**, *98*, 10465.
(13) Thompson, M. A.; Schenter, G. K. *J. Phys. Chem.* **1995**, *99*, 6374.
(14) Murphy, R. B.; Philipp, D. M.; Friesner, R. A. *J. Comput. Chem.* **2000**, *21*, 1442.
(15) Bernardi, F.; Olivucci, M.; Robb, M. A. *J. Am. Chem. Soc.* **1992**, *114*, 1606.
(16) Åqvist, J.; Warshel, A. *Chem. Rev.* **1993**, *93*, 2523.
(17) Singh, U. C.; Kollman, P. A. *J. Comput. Chem.* **1986**, *7*, 718.
(18) Štrajbl, M.; Hong, G.; Warshel, A. *J. Phys. Chem. B* **2002**, *106*, 13333.
(19) Stanton, R. V.; Hartsough, D. S.; Merz, K. M., Jr. *J. Comput. Chem.* **1995**, *16*, 113.
(20) Shaik, S.; Shurki, A. *Angew. Chem., Int. Ed. Engl.* **1999**, *38*, 586.
(21) Shurki, A. *Theor. Chem. Acc.* **2006**, *116*, 253.
(22) Warshel, A.; Weiss, R. M. *J. Am. Chem. Soc.* **1980**, *102*, 6218.
(23) Warshel, A. *Computer Modeling of Chemical Reactions in Enzymes and Solutions*; John Wiley & Sons: New York, 1991.
(24) Warshel, A.; Sharma, P. K.; Kato, M.; Xiang, Y.; Liu, H. B.; Olsson, M. H. M. *Chem. Rev.* **2006**, *106*, 3210.
(25) Chang, Y.-T.; Miller, W. H. *J. Phys. Chem.* **1990**, *94*, 5884.
(26) Chang, Y.-T.; Minichino, C.; Miller, W. H. *J. Chem. Phys.* **1992**, *96*, 4341.
(27) Grochowski, P.; Lesyng, B.; Bala, P.; McCammon, J. A. *Int. J. Quantum Chem.* **1996**, *60*, 1143.
(28) Schlegel, H. B.; Sonnenberg, J. L. *J. Chem. Theory Comput.* **2006**, *2*, 905.
(29) Kim, Y.; Corchado, J. C.; Villà, J.; Xing, J.; Truhlar, D. G. *J. Chem. Phys.* **2000**, *112*, 2718.
(30) Albu, T. V.; Corchado, J. C.; Truhlar, D. G. *J. Phys. Chem. A* **2001**, *105*, 8465.
(31) Lin, H.; Zhao, Y.; Tishchenko, O.; Truhlar, D. G. *J. Chem. Theory Comput.* **2006**, *2*, 1237.
(32) Vuilleumier, R.; Borgis, D. *J. Mol. Struct.* **1997**, *436*−*437*, 555.
(33) Vuilleumier, R.; Borgis, D. *Chem. Phys. Lett.* **1998**, *284*, 71.
(34) Schmitt, U. W.; Voth, G. A. *J. Phys. Chem. B* **1998**, *102*, 5547.
(35) Schmitt, U. W.; Voth, G. A. *J. Chem. Phys.* **1999**, *111*, 9361.
(36) Chakraborty, A.; Zhao, Y.; Lin, H.; Truhlar, D. G. *J. Chem. Phys.* **2006**, *124*, 44315.
(37) Garavelli, M.; Ruggeri, F.; Ogliaro, F.; Bearpark, M. J.; Bernardi, F.; Olivucci, M.; Robb, M. A. *J. Comput. Chem.* **2003**, *24*, 1357.
(38) Bearpark, M. J.; Boggio-Pasqua, M.; Robb, M. A.; Ogliaro, F. *Theor. Chem. Acc.* **2006**, *116*, 670.
(39) Mo, Y. R.; Gao, J. L. *J. Phys. Chem. A* **2000**, *104*, 3012.
(40) Mo, Y. R.; Gao, J. L. *J. Comput. Chem.* **2000**, *21*, 1458.
(41) Mo, Y. R. *J. Chem. Phys.* **2007**, 126.
(42) Hong, G. Y.; Rosta, E.; Warshel, A. *J. Phys. Chem. B* **2006**, *110*, 19570.
(43) Wu, Q.; Van Voorhis, T. *Phys. Rev. A* **2005**, *71*, 024502.
(44) Wu, Q.; Van Voorhis, T. *J. Phys. Chem. A* **2006**, *110*, 9212.
(45) Song, L. C.; Wu, W.; Zhang, Q.; Shaik, S. *J. Phys. Chem. A* **2004**, *108*, 6017.
(46) Shurki, A.; Crown, H. A. *J. Phys. Chem. B* **2005**, *109*, 23638.
(47) Mo, Y. R.; Song, L. C.; Lin, Y. C. *J. Phys. Chem. A* **2007**, *111*, 8291.
(48) Wesolowski, T. A.; Warshel, A. *J. Phys. Chem.* **1993**, *97*, 8050.
(49) Maseras, F.; Morokuma, K. *J. Comput. Chem.* **1995**, *16*, 1170.
(50) Lin, H.; Truhlar, D. G. *Theor. Chem. Acc.* **2007**, *117*, 185.
(51) Burton, N. A.; Harrison, M. J.; Hart, J. C.; Hillier, I. H.; Sheppard, D. W. *Farad. Discuss.* **1998**, *110*, 463.
(52) Hall, G. G.; Smith, C. M. *Int. J. Quantum Chem.* **1984**, *25*, 881.

(53) Smith, C. M.; Hall, G. G. *Theor. Chim. Acta* **1986**, *69*, 63.

(54) In VB/MM H_{ij} was approximated by the following equation. $H_{ij} = H'_{QM,ij} + (w_i H_{ii}^{int} + w_j H_{jj}^{int})S'_{QM,ij}$, where w_i and w_j are the weights of Φ_i and Φ_j respectively and $w_i = w_j = 1/2$ was used only in the special cases in which $H_{ii} = H_{jj}$. However, an in depth examination of the effect of using $w_i = w_j = 1/2$ instead of the actual respective weights was found to be negligible (see Supporting Information). Since using the weights requires several iterations to obtain their correct value, and since there is no clear justification for using the relative weights rather than equal average of the interactions, we decided to use the latter, which is the simpler version, here.

(55) The weights are fixed at this stage because in order to change them one should proceed with a quantum calculation as described in the subsequent steps. Since one step in dynamics is not expected to cause major changes in the weights, and since, within our method, one QM calculation is much more computer demanding than running several dynamics steps, we perform relaxation of the solvent to predetermined weights, then change the weights and repeat the relaxation until convergence is obtained.

(56) Song, L. C. W.; Wu, Y.; Mo, Zhang Q. XMVB-0.1—An ab initio Non-Orthogonal Valence Bond Program Xiamen University, Xiamen 361005, China, 2003.

(57) Wu, W.; Mo, Y.; Cao, Z.; Zhang, Q. A Spin Free Approach for Valence Bond Theory and Its Application. In *Valence Bond Theory*; Cooper, D. L., Ed.; Elsevier: Amsterdam, 2002; pp 143.

(58) Chu, Z. T.; Villa, J.; Štrajbl, M.; Schutz, C. N.; Shurki, A.; Warshel, A. *MOLARIS*, version beta9.05; University of Southern California: Los Angeles, 2004, in preparation.

(59) Lee, F. S.; Chu, Z. T.; Warshel, A. *J. Comput. Chem.* **1993**, *14*, 161.

(60) Hiberty, P. C.; Flament, J. P.; Noizet, E. *Chem. Phys. Lett.* **1992**, *189*, 259.

(61) Hiberty, P. C.; Shaik, S. Breathing-Orbital Valence Bond—A Valence Bond Method Incorporating Static and Dynamic Electron Correlation Effects. In *Valence Bond Theory*; Cooper, D. L., Ed.; Elsevier: Amsterdam, 2002; p 187.

(62) McWeeny, R. *Int. J. Quantum Chem.* **1988**, *34*, 23.

(63) King, G.; Warshel, A. *J. Chem. Phys.* **1990**, *93*, 8682.

(64) Burkert, U.; Allinger, N. L. *Molecular Mechanics*; American Chemical Society: Washington, DC, 1982.

(65) Roux, B. *Comput. Phys. Comm.* **1995**, *91*, 275.

(66) Muller, R. P.; Warshel, A. *J. Phys. Chem.* **1995**, *99*, 17516.

(67) Zwanzig, R. W. *J. Chem. Phys.* **1954**, *22*, 1420.

(68) Valleau, J. P.; Torrie, G. M. *Modern Theoretical Chemistry*; Plenum Press: New York, 1977; Vol. 5.

(69) Lee, F. S.; Warshel, A. *J. Chem. Phys.* **1992**, *97*, 3100.

(70) Song, L. C.; Wu, W.; Hiberty, P. C.; Shaik, S. *Chemistry—Eur. J.* **2006**, *12*, 7458.

(71) Hwang, J.-K.; King, G.; Creighton, S.; Warshel, A. *J. Am. Chem. Soc.* **1988**, *110*, 5297.

(72) Pellerite, M. J.; Brauman, J. I. *J. Am. Chem. Soc.* **1983**, *105*, 2672.

(73) Pellerite, M. J.; Brauman, J. I. *J. Am. Chem. Soc.* **1980**, *102*, 5993.

(74) Doughert, Rc; Roberts, J. D. *Org. Mass Spectrom.* **1974**, *8*, 81.

(75) Albery, W. J.; Kreevoy, M. M. *Adv. Phys. Org. Chem.* **1978**, *16*, 85.

(76) Chirgwin, H. B.; Coulson, C. A. *Proc. R. Soc. London, Ser. A* **1950**, *2*, 196.